



United States Department of the Interior

U.S. GEOLOGICAL SURVEY

Water Resources Division

520 N. Park Ave, Suite 221

Tucson, AZ 85719

smwiele@usgs.gov

(520) 670-6671 277

FILE COPY

February 27, 2003

MEMORANDUM

TO: Ted Melis, Physical Resources Program Manager, Grand Canyon Monitoring and Research Center

FROM: Stephen Wiele, Paul Grams, Peter Wilcock, Josh Korman, and Jack Schmidt

RE: First year progress report for the Grand Canyon Modeling project

We are working to produce two coupled sand transport and deposition models that will allow the effects of Glen Canyon Dam operations on sand storage to be evaluated. A one-dimensional model based on an existing flow model (Wiele and Smith, 1996; Wiele and Griffin, 1997) will be developed to route water and sand along the river corridor. An existing multidimensional model (Wiele and others, 1996; Wiele, 1997; Wiele and others, 1999, Wiele and Torizzo, in press) will be used to evaluate the effectiveness of a broad range of dam operation strategies in building high-elevation sand deposits. The models and their application will provide a physically-based predictive capability for management of Glen Canyon Dam releases and the Grand Canyon Colorado River corridor. Several issues critical to management are (1) the potentially rapid migration of tributary sand inputs through the system, (2) the relative efficiency of alternatives in the timing, magnitude, and duration of dam releases in building sand bars, and (3) the linkages between dam operations, sand deposits, and the biological, recreational, and archeological resources along the river corridor. The project includes several components that are critical for achieving an accurate and broadly applicable modeling capability: analyses of a database consisting of maps of sand-storage reaches to guide modeling site selection and application of modeling results, linkages to biological issues and models, and a new investigation of suspended sand transport over extremely rough boundaries with flume studies at the University of Minnesota St. Anthony Falls Hydraulic Lab, a critically important but poorly understood process that directly affects the accuracy of the models.

The majority of the modeling work in the first year involved refinements to and applications of the 2d model. The 2d model has been applied to several new sites chosen primarily because the bathymetry is available. Applications to the 30-mile site resulted in a presentation at Fall AGU

(Wiele and others, 2002) that demonstrated that short high flows make the best use of available sand in depositing high elevation bars, and also for a given volume of sand transported to the reach, use less water than lower (but still higher than power-plant capacity) discharge releases. Modeling focus will shift to the 1d model in the coming months to facilitate incorporation of flume study results.

The flume study component of the project has had a series of successful experiments and data reduction is ongoing. A sharp threshold in sand storage from a sand-covered bed to a sand-evacuated bed was observed, suggesting that between-rock sand storage is fragile and that sand entrainment may quickly blink out as a sand wave migrates through a reach. This result has significant implications for the role of interstitial sand storage on the channel bottom.

The project has had three meetings: a three-day meeting in Logan in March, 2002, a four-day river trip in September, 2002, and a brief meeting during AGU, December, 2002. The meeting in Logan involved detailed discussions of the structure of the 1d model and methods for extrapolating 2d model results to multiple depositional sites at a range of scales. The river trip focused on initial model results (at river mile 30, 43, and 45), flume studies, biological linkages, identification of modeling sites, and ongoing discussions of the extrapolation of modeling results. At AGU we met with Roberto Anima to discuss the progress and anticipated results of his sonar mapping of the channel bed. Roberto displayed images of the channel bottom that included maps of the textures overlaid in a GIS database.

The sections below present aspects of the project that have been the major focus of the work so far: model development and application, selection of modeling sites and flume studies of near-bed sand transport over a rough boundary.

Modeling Progress

Model revisions

The flow algorithm that was used before (Patankar, 1980) has been replaced with the Casulli (1992) Eulerian-Lagrangian method for shallow 2d flows. The Lagrangian component of the flow algorithm is primarily of interest for unsteady flow applications, but has demonstrated robust numerical characteristics. An additional advantage of the new implementation of the flow component of the 2d model is that it no longer requires the specification of the flow boundaries. Put another way, the current version will compute through dry nodes without problems. In the previous version of the model, wet nodes had to be specified. In the current version, the model computes over the entire mesh, returning trivial solutions at the dry nodes. The small loss in efficiency is offset by large improvements in the ease with which the model can be run. This arrangement also will allow for the simulation of unsteady flow, such as the rises and falls of discharge during BHBFs, with a series of steady flow solutions in kilometer-scale modeling reaches.

The new flow algorithm also seems to have contributed to faster runtimes. The runtimes have also been sped up by 2GHz computers (the Cultural resources project used mostly 400 MGz computers). The runtimes for this project so far, however, have also been decreased by applications to shorter reaches than were studied in the CR project. The runtimes for the slowest

cases (high discharge, high sediment loads) during the CR project took a week or more. The cases studied so far for this project have typically taken a few hours.

In the 1d model, the sand transport algorithm has been improved by adding advection to the suspended sand calculation. The previous version calculated a Rouse profile. This modification is intended to help alleviate a potential source of an erratic pattern of transport rates along the channel at a given time step and allow for longer time steps. The 1d model appears to exhibit smooth longitudinal patterns of sand transport if the bed is sand covered and the transport rates are high, but erratic transport if the sand level is below the top of the bed roughness. Smoother transport patterns at higher discharge are contrary to the authors' past experience with modeling sand transport, in that in general higher transport rates tend to be accompanied by greater volatility in the longitudinal stability as a result of continuity coupling. Although the greater sensitivity of sand transport to sand levels below the top of the roughness is represented in the 1d model with schematic algorithms, it mimics observations during the flume experiments of an abrupt transition between a sand-covered bed and a scoured condition despite the potential sheltering effects of the large roughness.

Gridding

A simple method of gridding bathymetry for the 2d model was developed that uses Tecplot software. Tecplot is a stable, supported 1, 2, and 3d plotting program based on software developed by NASA for presentation of fluid dynamics computations. Tecplot contours the bathymetric measurements and calculates a triangular mesh from which values at discrete points can be interpolated. It also has a utility that automatically interpolates points at locations listed in a file and returns a new file with locations and points. A separate utility program generates the point locations based on the upstream cross section locations and a downstream point which are obtained from a Tecplot utility. Tecplot is the same software that has been used in Wiele's projects to display contour plots of model results including flow vectors, stream lines, and animations of sand bar evolution.

Modeling sites and bathymetry issues

During the September river trip, we identified these sites as potential additional modeling sites: just below the Paria Riffle (already surveyed) -- data sent by Mark Manone (NAU)

Cathedral (rm 2.5; already surveyed) -- sent by Mark Manone (NAU)

22 mile (FIST reach) -- listed as processed by GCMRC, but not delivered to GIS

Silver Grotto (rm 29) -- listed as processed by GCMRC, but not delivered to GIS

RM 31 -- data received from NAU

Reaches within rm 42-45 -- available on GCMRC web site

Saddle (rm 47.2) -- surveyed on May 2001 trip by GCMRC, not processed

55 mile -- surveyed May 2002 trip by GCMRC, not processed

60 mile -- surveyed May 2002 trip by GCMRC, not processed

Sites simulated will be restricted by available bathymetry. Bathymetry between the confluence with the LCR and Upper Unkar is available for nine sites from previous modeling projects. Bathymetry at sites surveyed during the '96 release has been provided by Ned Andrews and are good candidates for simulation, although there is limited control on sand transport and grain size. Additional bathymetry will apparently only be available from the NAU monitoring project. NAU has already provided bathymetry below the confluence with the Paria River.

Model application

The model has been applied to three new locations: 30-mile and two sites using the river mile 42-45 bathymetry. For the sites at 30-mile and 45-mile, the NAU Sand Bar Studies group provided minimum bed bathymetry that they synthesized from their numerous surveys at those sites. Modeling results described in this section for 30-mile are derived from a presentation at fall AGU titled *The significance of discharge in the replenishment of sandbar deposits along the Colorado River through Grand Canyon* by S. Wiele (U.S. Geological Survey, Tucson AZ), J. Hazel (Northern Arizona University), J. Schmidt (Utah State University), and T. Melis (U.S. Geological Survey, Flagstaff, AZ). The presentation combined modeling results and data from the NAU Sand Bar Studies to conclude that for a given sediment supply, flows greater than power-plant capacity (PPC) build larger bars at higher elevations, where they last longer, require less time to build the bars, and use less water. For this progress report, most of the background material has been removed and only the model component is described.

Flow, sand transport, and bed evolution were modeled for conditions that occurred during PPC flows and at five bypass discharges. Modeling results show that bypass discharges form larger, higher-elevation deposits than are possible at PPC discharges. Key requirements for substantial deposition of new sand along the sides of this narrow, deeply incised river are sufficient fine-sediment supply and the availability of suitable depositional sites. The use of PPC releases for building substantial sandbars is complicated by their high efficiency at exporting channel-bed sand while accessing limited accommodation sites where deposition can occur, as shown by sand-transport data collected from 1997-2000. Under enriched sediment-supply conditions, transport rates for sand is increased under PPC flows, while accommodation sites for deposition remain limited. Results to date indicate that restoration and maintenance of sand bars will likely require releases greater than PPC more frequently and of shorter duration than anticipated in the past.

The multidimensional model of flow, sand transport, and bed evolution (Wiele and others, 1996; Wiele, 1997; Wiele and others, 1999) was applied to a reach that was studied during a power plant capacity release in 2000. The model has been applied to large-scale events, such as the effects of major tributary flooding on main stem sand deposits and the 1996 experimental release, and shown to agree well with measurements of cross sections and channel surveys, predicting accurately both the volume and location of sand deposits. The power-plant capacity discharge, however, provides a particularly challenging application for the model in that it was a

relatively mild event with a small response of the sand bars relative to the large-scale events modeled previously.

The study reach, located near 30-mile is of particular interest because it is located relatively close to the dam, and hence is subject to the consequences of typical, lower sand supply, and contains sand deposits that are relatively large for that section of the river below Glen Canyon Dam. During the release, suspended sand was measured at the upstream end of the reach (David Topping, USGS, written communication, 2000) and the channel shape was surveyed once or twice each day of the 3-1/2 day events (Northern Arizona Sand Bar Studies, written communication, 2000).

Comparisons of model predictions with surveys is complicated by the apparent slumping of deposits, a process not contained in the model. Losses of large proportions of fresh sand deposits during the 1996 test release were attributed to slumping (Andrews and others, 1999). During the 2000 power-plant release, sudden loss of sand was especially apparent during the first day. The model has consistently shown good agreement with bathymetry measured during periods with no apparent slumping, especially during large-scale events such as the '96 release and the '93 flood on the LCR, but the occurrence of slumping confounds the comparison of model results with data and the general application of model results to hypothetical events. Incorporating the effect of slumping in the model results is constrained by limited data. One approach is to establish a method for empirically accounting for estimates of the effects of slumping that incorporates current information and that can be refined with new measurements. For the model application to 30-mile, the bathymetry and sand flux starting on the second day was used as the initial condition.

Model predictions of deposition are close to surveyed deposition over the first day of the simulation (Fig. 1m).

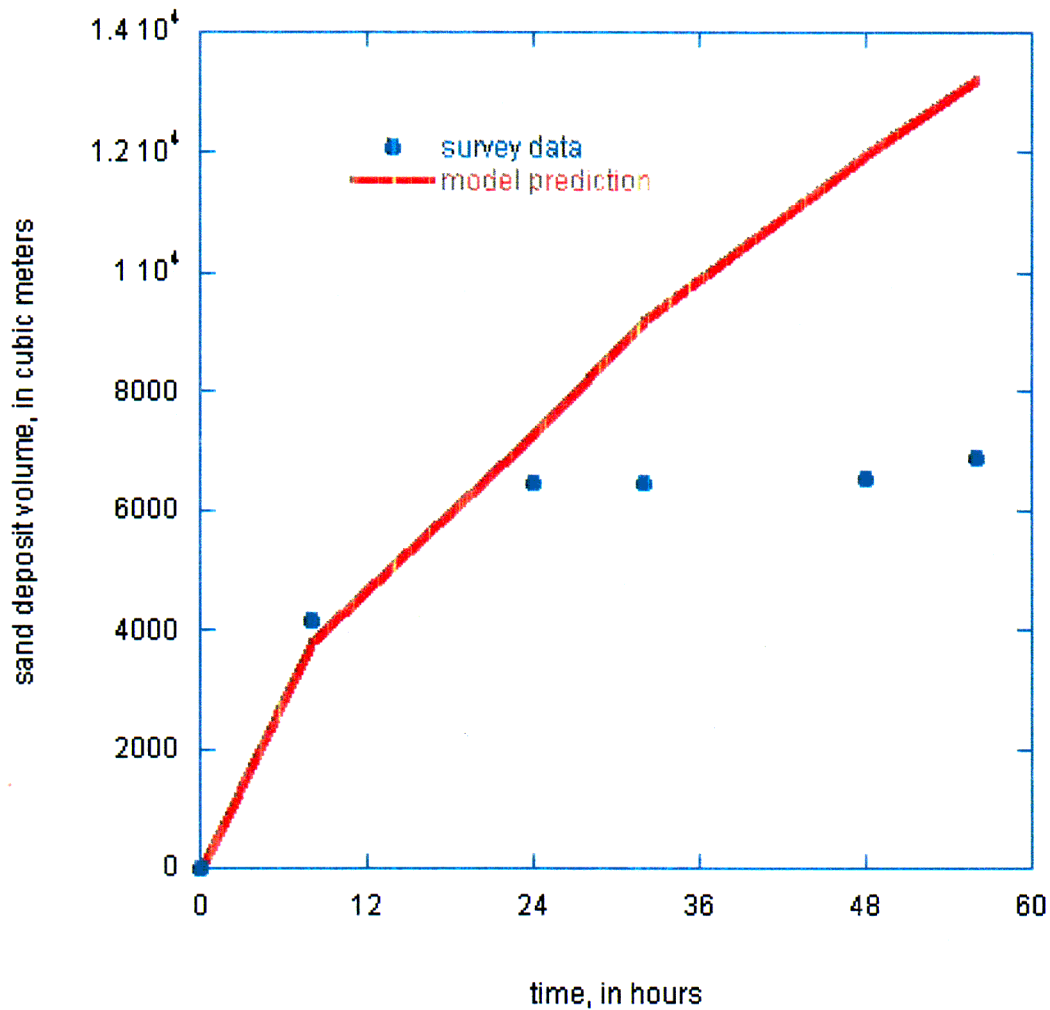
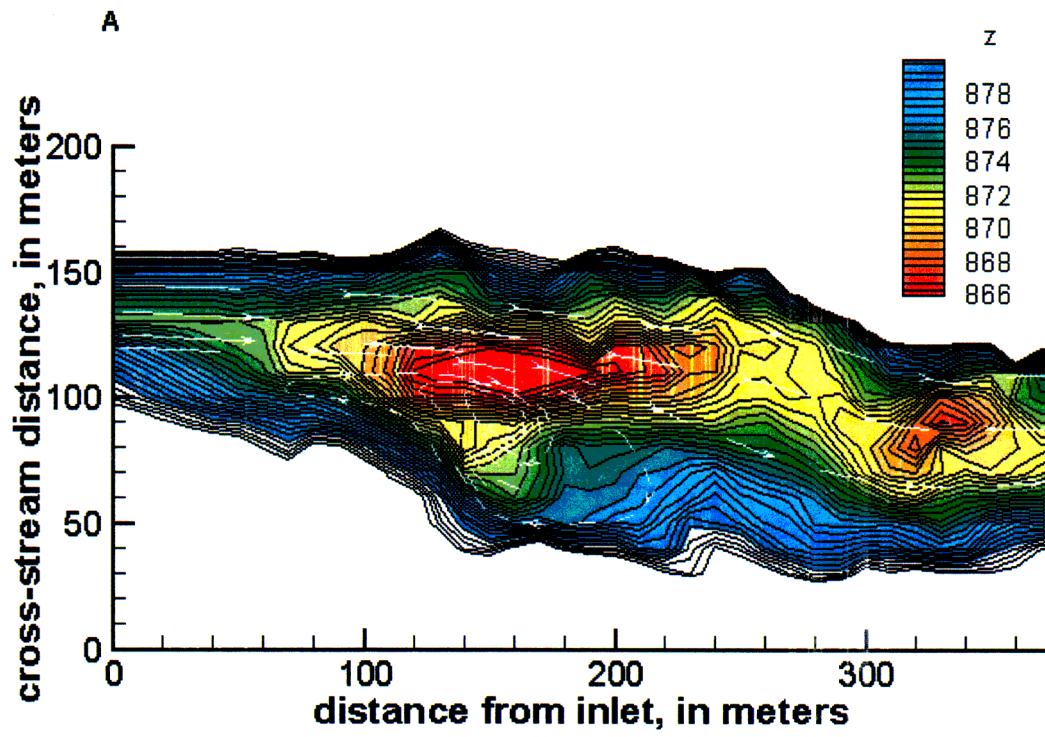
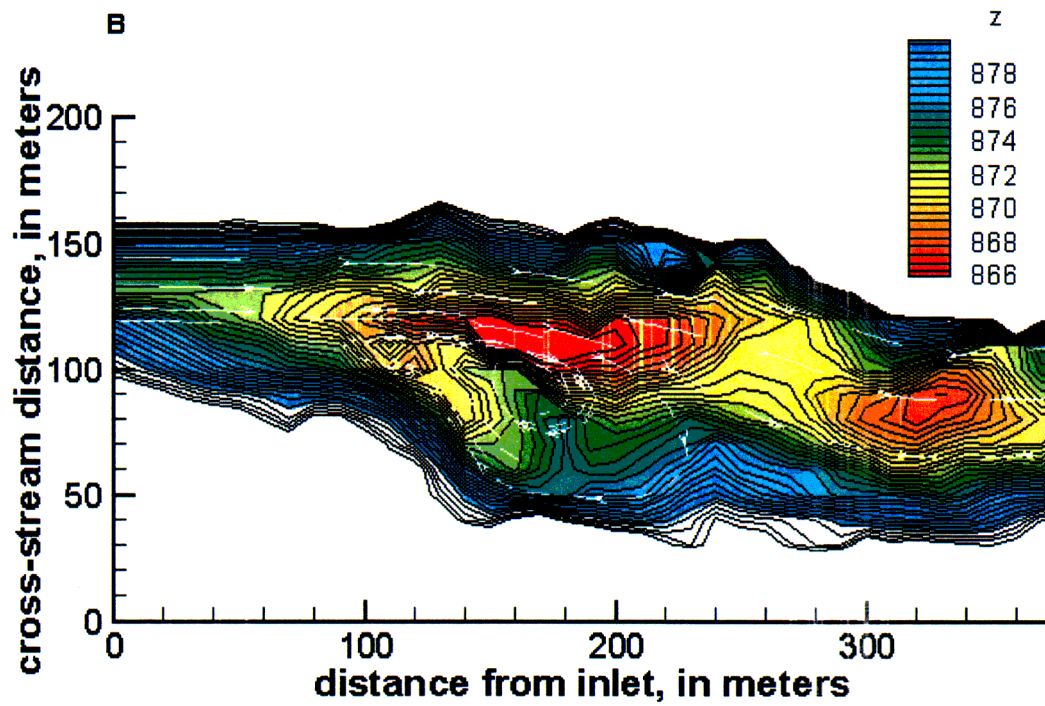


Figure 1m. Sand deposition near the recirculation zone determined from surveys and predicted by the model.

The overprediction by the model of deposition after the first day may be a result of ongoing slumping. The model predicts that most of the deposition would occur within the recirculation zone whereas the survey shows the reattachment point as the focus of deposition (Fig. 2m).





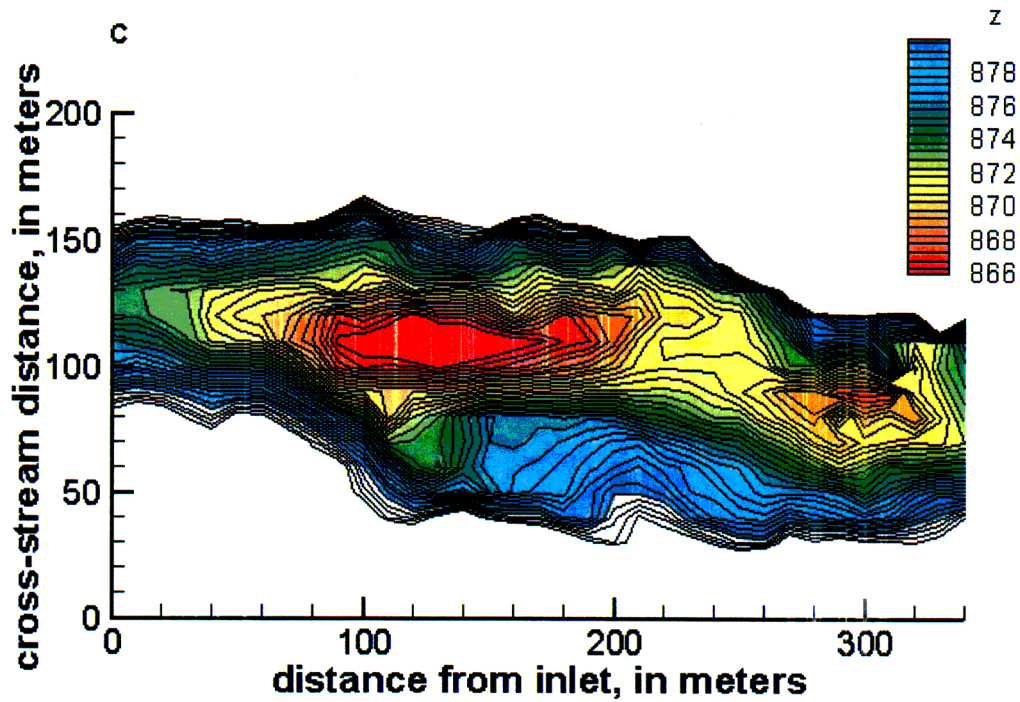


Figure 2m. Contour maps of the 30-mile reach showing (a) the initial channel shape used in the model, (b) the channel shape after 24 hours predicted by the model, and (c) the channel shape surveyed about 1 day after the survey shown in (a). The contour interval is $\frac{1}{2}$ meter. Flow is from left to right.

Sensitivity tests show model places sand at reattachment point if the grain size is coarser than the measured d50. The disparity between the model and the survey may be a consequence of the use of a single grain size in the model.

We also applied the model to five discharges greater than power-plant capacity to examine the relative efficiency with which sand bars could be deposited at various discharges for a given sand supply. Measured sand flux during the 2000 event showed a much higher sand concentration following the start of the sustained high flow that tapered down to a nearly steady flux. We used the relatively steady flux after the second day as input to the model at power-plant capacity for this comparison. At higher discharges, we extrapolated using the sediment rating curves developed by Topping (USGS, written communication, 1998; Fig. 3m).

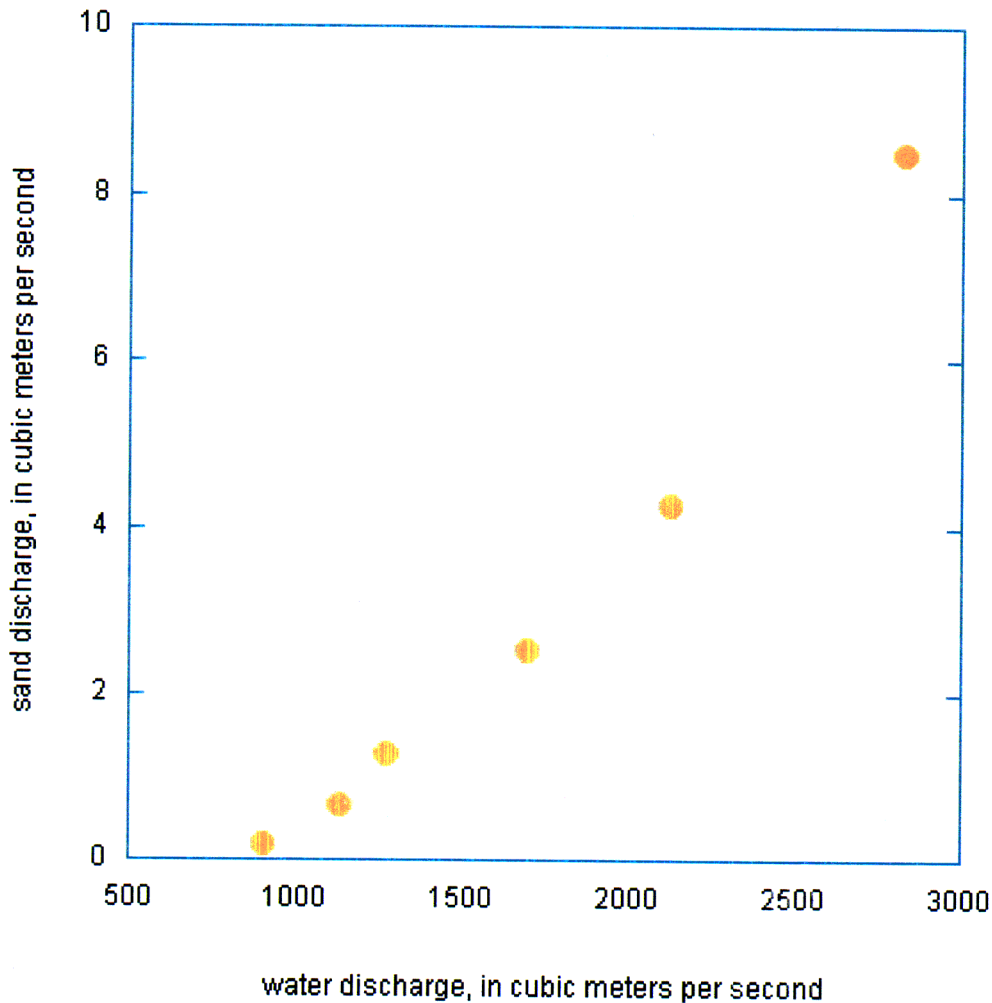


Figure 3m. Sand discharges used in the model application.

Topping developed a family of sediment rating curves for various sand supplies based on measurements at the Grand Canyon gage. Our study site is about 90-km upstream from the Grand Canyon gage, but the sand transport rate for a given sand supply and water discharge is likely sufficiently similar to warrant their use for this comparison.

Stage at each discharge was determined from a rating curve developed from surveys at known discharges up to about $1270 \text{ m}^3/\text{s}$ (Northern Arizona University Sand Bar Studies, written communication, 1998). The rating curves were extrapolated up to $2,830 \text{ m}^3/\text{s}$ using the method of Wiele and Torrizo (submitted for Director's approval).

To compare the relative efficiency with which various discharges deposit sand for a given sand supply, we computed the length of time required for each discharge to transport the volume of sand transported during the 2000 event (Fig. 4m). (The total time at $906 \text{ m}^3/\text{s}$, 108 hours, is longer than the 2000 event because we used a constant transport rate for the model applications that was characteristic of the transport rates after the initial sand transport peak.) We designate this time T_v .

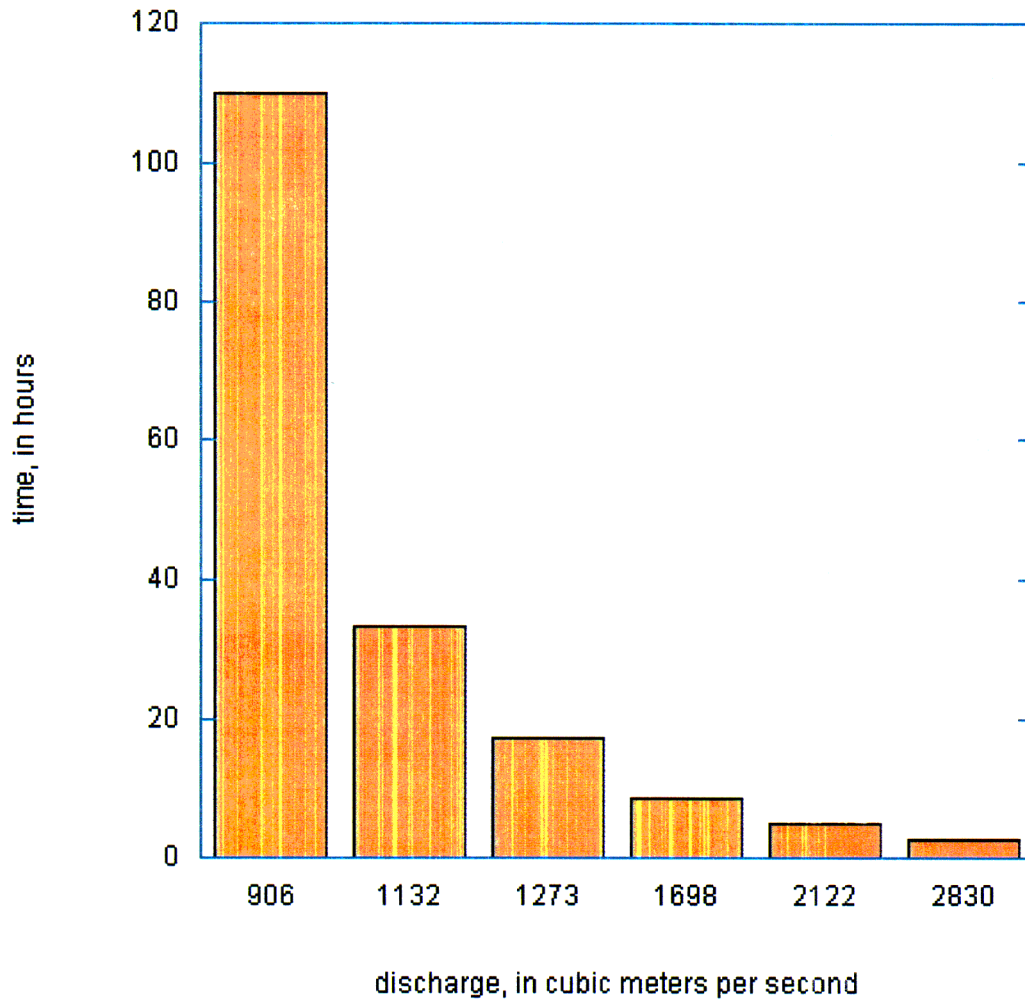


Figure 4m. The length of time for each modeled discharge to transport a volume of sand equal to the volume transported during the 2000 event.

The model predicts that higher discharges produce larger deposits than the lowest discharge as a function of time. The three lowest discharges produce nearly equal total deposit volumes that are greater than the higher discharges, however, at time T_v . Deposition rates are proportional to water discharge, but the high sand transport rates at the higher discharges lead to small values of T_v .

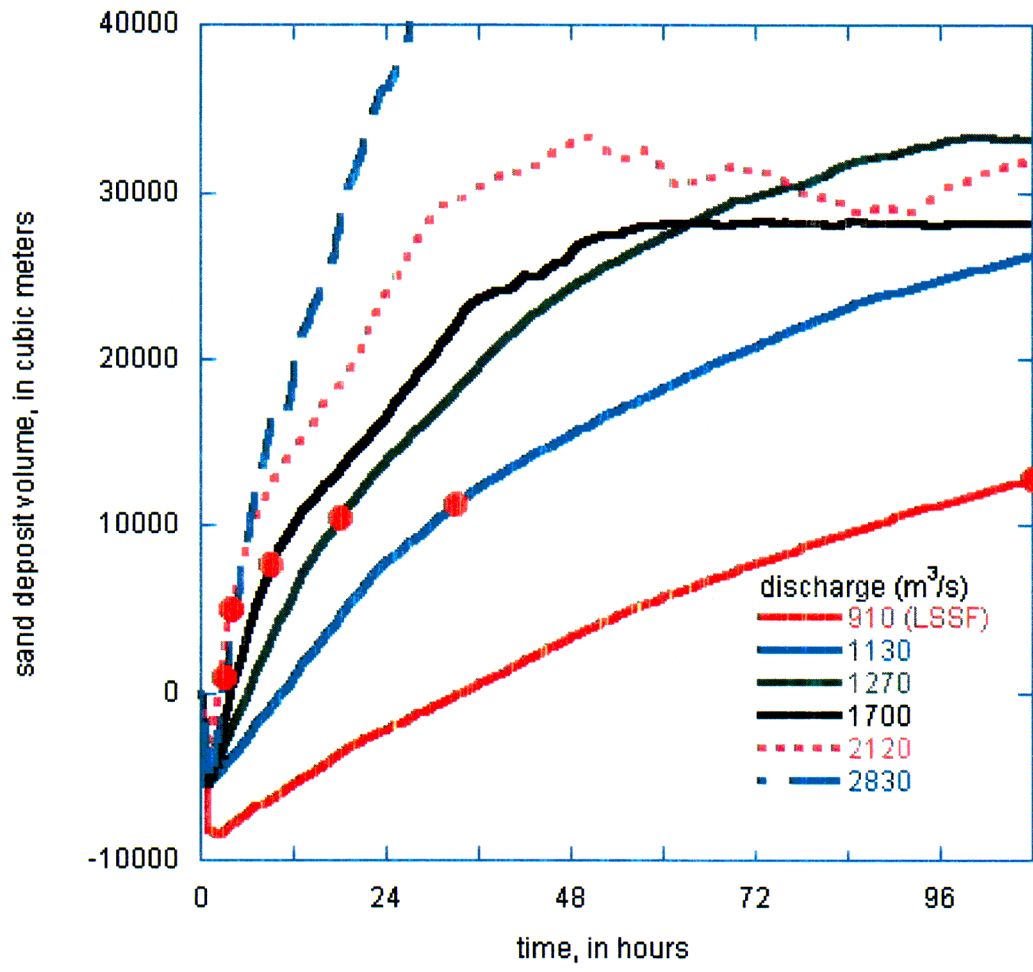


Figure 5m. Total sand deposition near the recirculation zone predicted by the model. The red discs mark the time at which a volume of sand equal to the volume of sand transported during the 2000 event has been transported by each discharge.

An important consideration in planning dam releases to maintain sand deposits is the likely longevity of these deposits. Deposits at higher elevations that are not subject to erosion by water are likely to last longer than lower deposits. Model predictions show that the short, high discharges are more effective at producing high elevation deposits, deposits at an elevation higher than the 708 m³/s stage (Fig. 6m). The high elevation deposition at 2830 m³/s is slightly lower than the peak volume at 2120 m³/s, and declines as discharge declines.

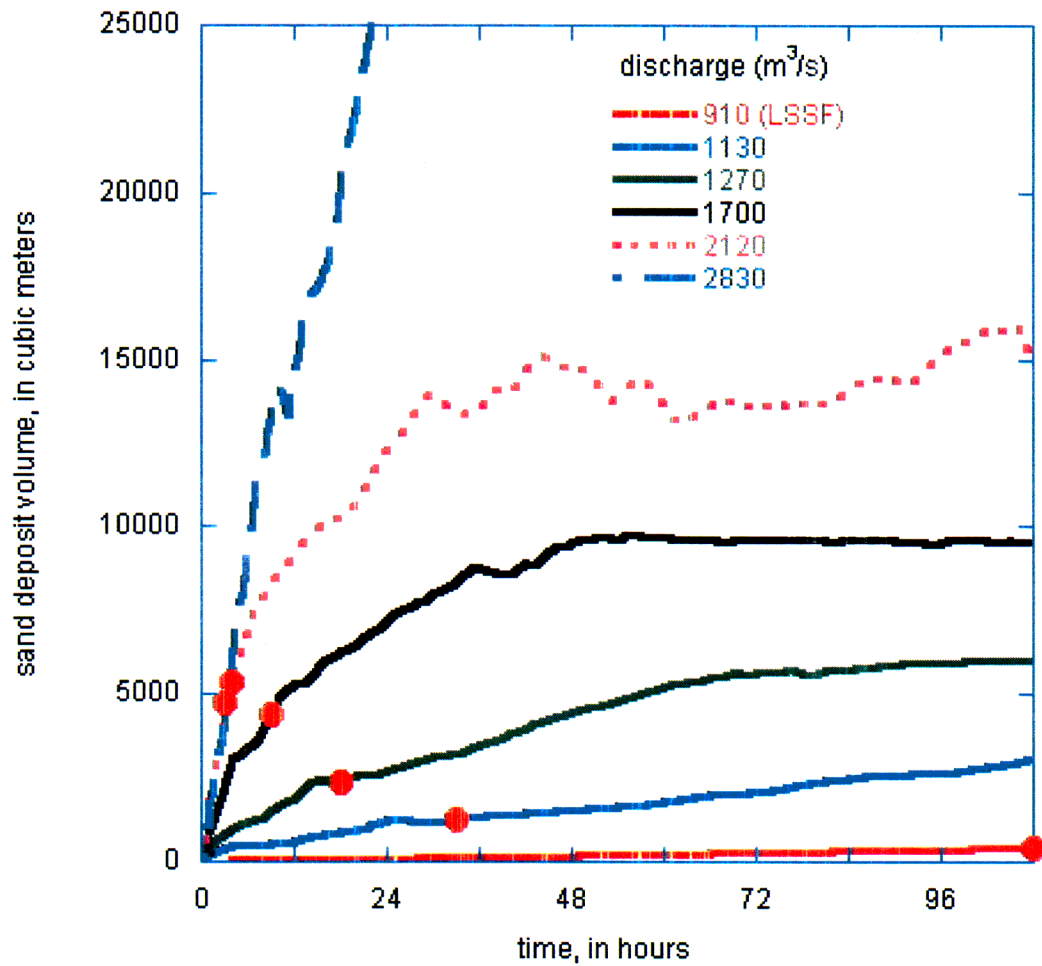


Figure 6m. High elevation sand deposition near the recirculation zone predicted by the model. The red discs mark the time at which a volume of sand equal to the volume of sand transported during the 2000 event has been transported by each discharge.

The greater efficiency with which high discharge produce high elevation deposits is largely a result of the associated higher stages (Fig. 7m) as well as the higher sand concentrations in suspension at higher discharges.

Fig

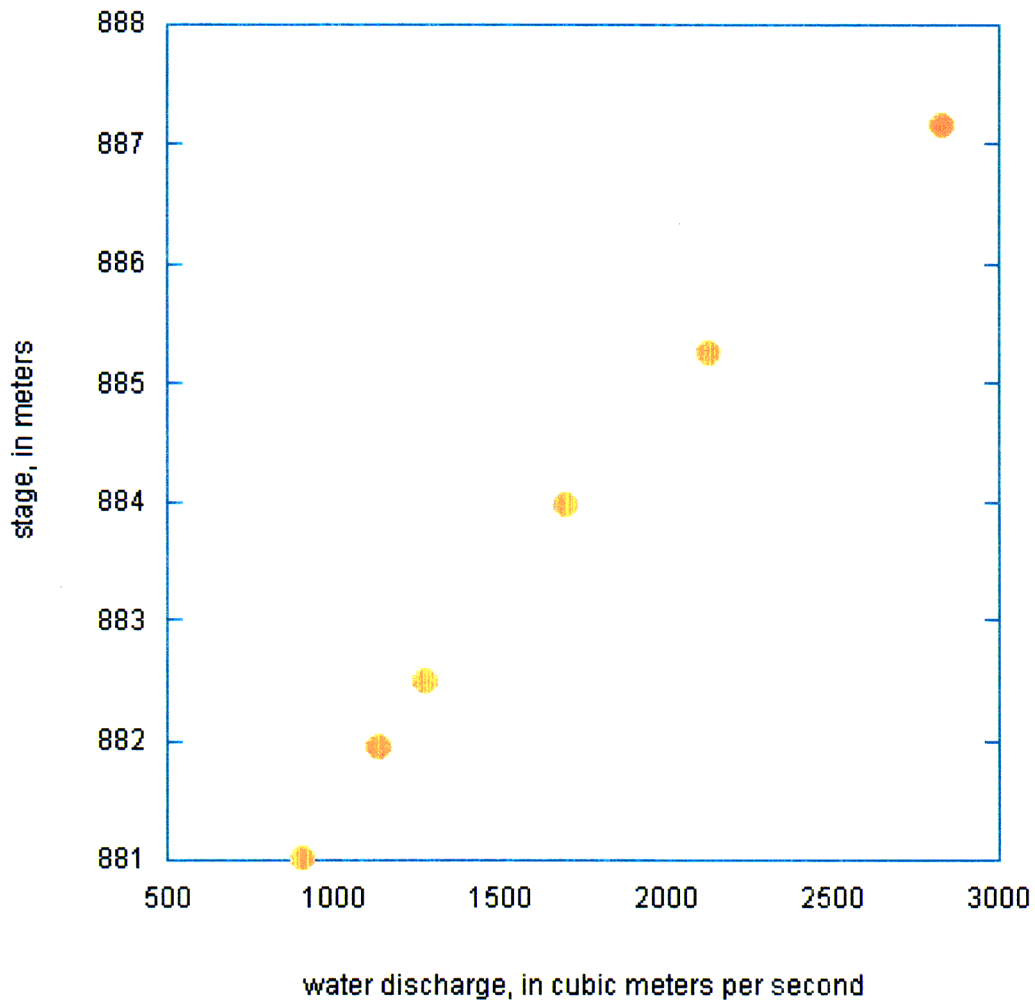


Figure 7m. Stage at each simulated discharge.

Another important issue in the planning of dam releases for the maintenance of sand deposits is the volume of water used, especially for the bypass releases. Except for the highest discharge, all of the discharges higher than power plant capacity used about the same volume of water in excess of power plant capacity before time T_v was reached (Fig. 8m.) The volume of water computed using discharges greater than $226 \text{ m}^3/\text{s}$ decreases as the discharge increases.

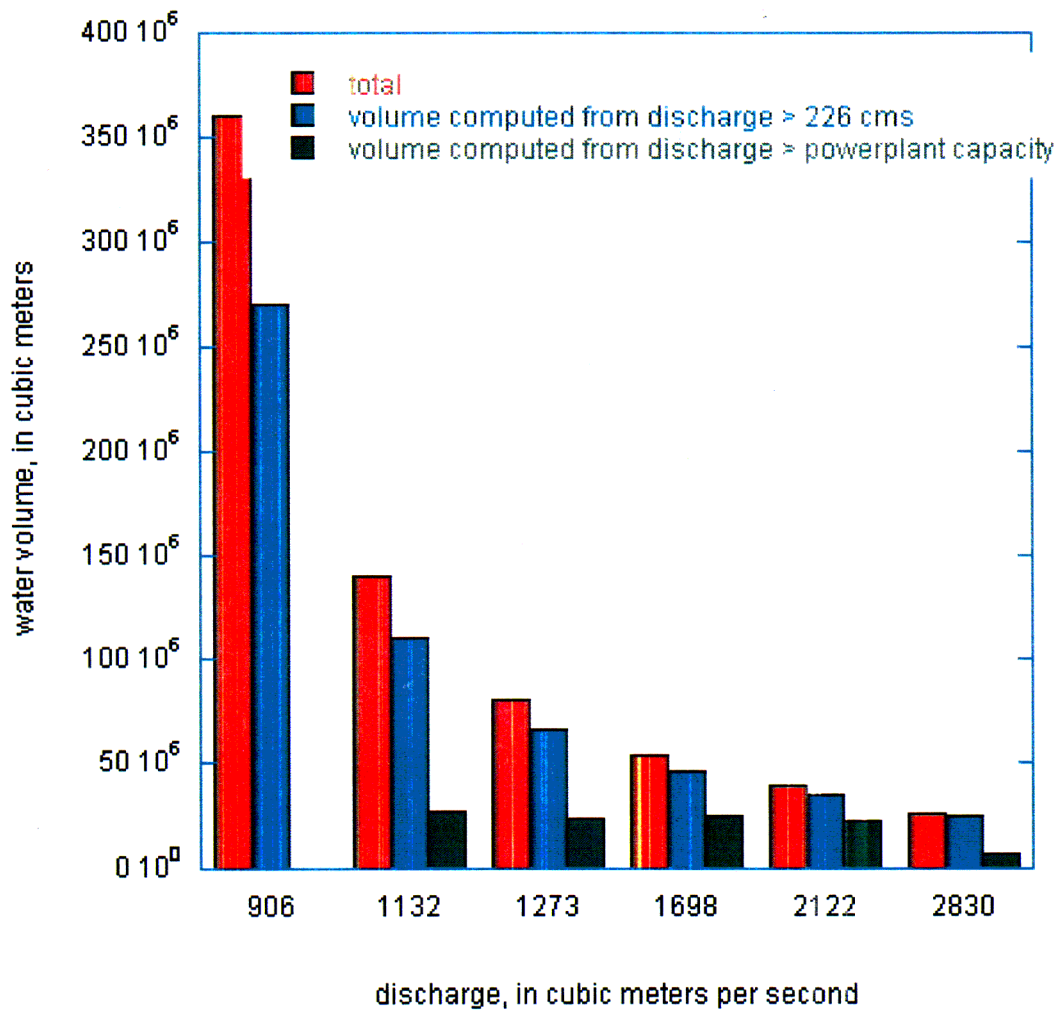


Figure 8m. Volumes of water released during the time interval T_v for each modeled discharge.

Surveys and mapping of sand bars and past applications of the model to other sites and conditions have shown that the response of sand bars to different discharges and sand supplies varies with local channel morphology. Consequently, we are proceeding with studies similar to the one presented here at other sites. Results so far suggest that high discharge, short duration releases are most effective at producing sand deposits that are more persistent over time than lower elevation deposits.

A key element in constructive dam releases, especially with high discharges, is an adequate sand supply. Long-term sand storage under normal dam operation may be inadequate to build sand

bars close to the dam (Topping and others, 2000a, 2002b; Rubin and others, 2002). Sand availability is the subject of ongoing research into sand fluxes and high-resolution measurement methods (Melis and others, 2002a, 2002b).

Eddy characteristics

The dominant topic during the project river trip in September was how to accommodate the variability in eddy sand storage in the model, and how to extrapolate from modeling sites to eddies at other locations and with different morphologies and channel characteristics. The discussion centered around the USU work on historical sand storage changes and associated geomorphic insights. The outcome of the September river trip discussions was that it would be reasonable to start with assumption that sand accumulation for a given set of conditions is proportional to eddy area. The MPAEBs calculated by USU have been based on total sand area and have included archaic sand deposits that are presently inactive. These areas, which will be used to normalize area for extrapolation of model results, are currently being recalculated to include only active sand area.

Flume studies of near-bed sand transport over a rough boundary

A critical component of the reach-averaged sand routing model is a sub-model for the prediction of the near-bed sand concentration. Although a variety of models for sand entrainment exist, all have been developed for situations in which the bed material and the material available for transport belong to the same size distribution. Application of these models to the problem of sand entrainment over a bed composed of larger roughness elements has not been tested. The objective of these laboratory flume experiments is to collect data that will allow us to test and modify, if necessary, existing models to sand entrainment over coarse beds.

Description of experiments

The flume experiments were conducted in a 14 m long by 1 m wide tilting-bed flume located at the Saint Anthony Falls Hydraulic Laboratory at the University of Minnesota. Flume preparation took place in June and the experimental runs were made between July 11 and August 3, 2002. To create a uniform coarse roughness, we covered the bed with 10 cm diameter polypropylene plastic hemispheres. The hemispheres were glued to a plastic false bottom in a "closest packing" arrangement, such that sphere tops were not aligned but staggered (Figure 1). The hemispheres covered the flume bed for a length of 12 m beginning 1.5 m below the headbox. The hemispheres were painted to facilitate visual observations of the sand-bed elevation. The upper 1.7 cm of each hemisphere was painted black, the middle 1.8 cm yellow, and the bottom 1.4 cm was left unpainted (white). Fine sediment was fed into the upstream end of the flume through a 10 cm diameter plastic pipe positioned immediately upstream from the first row of hemispheres. A constant feed rate was maintained by an automated sediment feeder (Runs 11-16) or by continuously pouring small containers of known volume into the pipe at timed intervals (all other runs).

A flow depth of 0.45 m was selected to provide sufficient depth above the roughness elements to allow observation of both a near-bed spatially variable layer and a thicker, spatially averaged layer in the core of the flow. To provide adequate velocity with the available discharge, we

reduced the working width to 0.3 m by constructing a false plywood wall along the length of the flume. Actual flow depth during runs varied from approximately 44 to 46 cm. The bed slope was 0.0006 for all runs.

We completed a total of 18 experimental runs, which are divided into three different run configurations. In the main or "F110" runs, sand with a median diameter of 0.12 mm (US Silica F-110 Ottawa Foundry Sand) was fed at rates between 33 g/s and 200 g/s using water discharges between 53 l/s and 98 l/s (Table 1). Each run was started with a clean bed (no sand in the spheres) and run times were determined such that the total volume of sand fed exceeded the maximum available bed storage by a factor of three or greater. For the final 2 to 5 minutes of most of the F110 runs, the sand feed was replaced with a colored sand feed of the same size, to allow observations of sediment mixing within the bed. In the coarse sand or "Lakeland" runs, a wider size distribution in the sand was achieved by using a mixture consisting of 1 part 0.3 mm median diameter sand and 2 parts F110 sand. Run times were determined as for the F110 runs and colored sediment was not used.

In the third run configuration, an initial bed was seeded to an elevation even with the hemisphere tops along a 2 m segment from 6 m to 8 m downstream of the head box. For two of these runs, the seed segment was divided into two 1-m sections each consisting of two layers of F110 sand of different colors. The 6 to 7 m section had 2.5 cm of red sand covered by 2.5 cm of green sand, and the 7 to 8 m section had 2.5 cm of yellow sand covered by 2.5 cm of blue sand. In these colored bed runs, the feed sediment was uncolored white F110 sand. The goal of this run was to examine the longitudinal and vertical pattern of sand entrainment from the bed and the source of transported sediment (entrained from the bed or fed at the headbox) sampled downstream. In the third seeded-bed run, the 6 m to 8 m segment was filled to the hemisphere tops with the coarse mix, which was also used as the feed sediment.

For each run, we measured flow, collected samples of suspended sediment, and recorded the post-run bed topography. The inflow rate was measured by a Pitot tube in the water supply line, which we calibrated by weighing the mass outflow for timed intervals. Water surface elevations were recorded at 1 m intervals along the length of the flume and monitored throughout each run for uniformity.

Samples of suspended sediment were collected at one sampling location 10.5 m downstream from the flume headbox (Figure 2). This location was chosen because it was well downstream from any entry effects caused by the flow contraction exiting the headbox and the beginning of the rough bed at the head of the flume. Samples were drawn from the flow by a rake of stainless steel Pitot tubes with nozzles positioned at elevations of 0.5, 2, 5, 10, and 30 cm above the hemisphere tops. Each Pitot tube was attached to a length of plastic tubing that carried the sample to a collection jar. Prior to sampling the suspended sediment, point velocities at each sampling location were measured with an acoustic Doppler velocimeter (ADV; SonTek 10-MHz). Velocity through the sampling tube was adjusted to match that of the local flow by adjusting the elevation of the siphon tube outlet. Between one and five sets of suspended sediment samples were collected for each run and sample durations ranged from 30 to 60 s. A total of 294 suspended sediment samples were collected and analyzed for sand concentration. All samples have been retained for analyses of grain size and proportions of colored sand where relevant.

For each of the flow rates used in the experimental runs, a set of detailed velocity measurements was made with the ADV. Velocity profiles were measured directly over a hemisphere top in the center of the channel at the sediment sampling location and on the right side of the channel one row downstream from the sampling location (Figure 2). A third profile was collected over the gap between two spheres one row downstream from the sediment sampling location. For one flow rate, centerline velocity profiles were collected at 1-m intervals along the length of the flume. Each profile consisted of seven velocity measurements made 0.5, 1.0, 2.0, 5.0, 10.0, 20.0, and 30.0 cm above the height of the hemisphere tops. Individual velocity measurements were collected at a 25 Hz sampling rate for a period of one minute. The ADV measures velocities in three orthogonal coordinates within a sample volume that is approximately 0.2 cm^3 located 5.1 cm below the probe tip.

Following each run, the entire length of the hemisphere-covered bed was photographed from directly above in 0.5 m sections. The depth of sand was measured directly along the centerline and along each sidewall at 69 evenly spaced positions. The depth of colored sand was also measured at each of these locations for runs in which colored sand was used. For the seeded-bed runs, in which four colors of sand were used, the remaining deposit was described in greater detail. Bed samples were collected at approximately 2-m intervals along the flume bed. Separate surface and sub-surface samples were collected where there was a difference in surface and sub-surface grain size or sediment color.

Interim Results

Bulk transport and bed deposition

The experimental procedure for the uniform transport runs with both the F-110 and coarse sediments was to begin with chosen sediment feed rate, than proceed with a series of runs to establish a flow rate that produced a uniform sediment bed and transport field. In our first four runs (Runs 0-3), we discovered that, for the feed rate of 75 g/s, there was a very narrow range of flows for which a stable bed would form. For larger discharges, all of the sediment would remain in suspension and no sand bed would form (Figure 3). For smaller discharges, sediment would accumulate rapidly on the bed, usually beginning about 3 to 4 m downstream from the headbox, and migrate downstream as a coherent dune that increased in height and length as it moved downstream (Figure 4). Over a narrow range of discharge, sand would accumulate in the hemisphere interstices and the average depth of sand down the centerline of the flume would be significantly greater than zero and less than the 5 cm height of the hemispheres (Figure 5). However, even in the runs for which the mean sand bed elevation was below the sphere tops, sand would develop local accumulations above the sphere tops. This deposition occurred along the edges, driven by reduced velocity and bed shear near the wall, and in scattered patches of sand (Figure 6). Following these initial observations, a primary focus of the experiments was to perform runs within the narrow discharge/sand feed range that produced a "target" bed: appreciable sediment retention on the bed without massive bed aggradation and dune formation.

The target bed conditions were achieved for F110 sediment feed rates of 33, 41, 75, and 200 g/s, corresponding to mean concentrations of 560, 617, 1130, and 2169 mg/l, respectively. Target

bed conditions were achieved for coarse sediment feed rates of 20, 43, 46, and 179 g/s, which correspond to mean concentrations of 301, 606, 579, and 1925 mg/l, respectively. Results, categorized by bare bed, target bed, and dune formation are summarized in Figure 7. For the F-110 sediment, the narrow range of flow rates producing a target bed was bracketed over a range of discharges using sediment feed rates of 75 g/s and 200 g/s.

The narrow range of discharge producing a target bed for a given sediment feed rate suggests that the stage of sand within the interstices of coarse roughness elements is rather fragile. We presume that wakes shed by the roughness elements rapidly evacuate fine sediment from the interstices when flow is able to separate over the sphere tops. Mark Schmeckle attempted to film this process using high speed video and laser sheet illumination, but poor water clarity prevented successful image acquisition. The discharge required to produce a target bed for the coarser Lakeland sediment is consistently larger than that for the F-110 sediment (Figure 7).

Velocity Field

We analyzed the velocity measurements to construct profiles of mean streamwise velocity and estimates of Reynolds stress based on the turbulence characteristics. Figure 8 shows velocity profiles for the location over the hemisphere top at the sediment sampling location (Station 1) and Figure 9 shows the profiles at the location over the interstices (Station 3). The horizontal error bars show the magnitudes of the streamwise turbulence intensities. The turbulence intensity is given by

$$\sqrt{\overline{u'^2}}$$

where u' is the instantaneous velocity,

$$u' = u - \bar{u}$$

u is the instantaneous streamwise velocity, and \bar{u} is the time-averaged streamwise velocity. Most of the profiles have a straight (in semi-log space) or nearly straight segment above 2.0 cm elevation. The lower segment (0.5 to 2 cm) is more variable and presumably dominated by wakes shed by upstream spheres. In some cases, the lower segment is an extension of the upper logarithmic segment or defines a separate straight line on the semi-log plot. In other cases, the velocities in the lower segment are nearly constant throughout the lower 2 cm of the profile.

Sediment Concentration Profiles

One of the motivations for these experiments is to evaluate near-bed sediment concentrations for suspended sediment flows over coarse bed topography. Although the reference elevation for the near-bed concentration is usually taken to be very near the bed, typically scaling with the grain size of the sediment in transport, application to a transport condition with two very different sediment length scales is more complex. Figure 10 shows our measured concentrations and a Rouse profile for a reference elevation of 0.5 cm above the hemisphere tops. Figure 11 represents the same data using a reference elevation of 2.0 cm. When 0.5 cm is used as the reference elevation, the Rouse profile underpredicts the concentrations at higher elevations. In all cases, including F-110 and coarse sediment feeds, using 2.0 cm as the reference elevation provides a much better match between the predicted and measured concentration profiles. Determination of the most useful near-bed reference elevation from which sediment is diffused into the core of the flow is one element of our model evaluation.

Figure 12 shows sediment concentration at a height of 2.0 cm as a function of shear velocity u^* as determined from the Reynolds stress computed from turbulence measurements at the same elevation. Concentrations are smaller for the coarser "Lakeland" mix. Concentrations are also smaller when the mean bed elevation is lower. These results are part of the data that will be used to test the near-bed concentration computations within the reach-averaged transport model.

Planned Work Year 2

Work planned for year 2 of the project includes completion of the data reduction and analysis and testing of the suspended transport model to be used in the 1-d sand routing model. Data analysis tasks are summarized in Table 2. The largest remaining data reduction task is size analysis of the suspended transport and bed samples. In processing the ADV data, we have noticed occasional significant errors (principally large negative streamwise velocity; e.g. Figure 9, Run 10). We will, therefore, filter the ADV data and recalculate velocity statistics. Once the near-bed concentration data are complete, we will be able to test the proposed algorithm for computing near-bed sand concentration.

Principal Findings

The 2002 flume runs were successful. We were able to conduct more flume runs than originally proposed. An equilibrium transport field was established using two sediments with different grain sizes and for a range of discharge and concentration. We successfully measured the flow, transport, and bed properties needed for test the suspended transport model. Supplemental observations using colored sand, introduced either at the end of a run or in layers placed in the bed of the flume, will provide qualitative observations that will help in evaluating our transport model.

An unanticipated result of the flume runs was the very narrow range in discharge and sediment concentration that produced a sediment bed with an elevation at or below the tops of the large roughness elements. For a given sediment feed rate (and concentration), if the discharge was larger than this range, nearly all sediment remained in suspension, with little or no sediment stored on the bed. If the discharge was slightly smaller than this range, sand accumulation on the bed was rapid and migrating dunes formed. This narrow range suggests that there is a threshold combination of discharge and sand concentration below which sand accumulated on the bed can be rapidly evacuated.

The implications of this observation may be illustrated by considering a sequence of events beginning with widespread sand deposition in a reach, followed by progressive removal of sand under conditions of negligible sand supply. Our results suggest that once the sand bed elevation begins to fall below the tops of the large roughness elements, eddies in the wake of the roughness elements can act to entrain most of the remaining sand from within the interstices among the large grains. This suggests that preservation of tributary derived sand in the bed of the Colorado River may depend critically on maintaining a relatively pervasive sand cover. Once this cover is broken, rapid excavation of sand from among the roughness elements may leave little sand available for further transport.

In terms of modeling the migration of a sand wave through the Colorado River in the Grand Canyon, an implication of this work is that the sand entrainment and transport in a reach may

rapidly shift from a large value corresponding to a sand bed to a very small value corresponding to absence of transportable sand on the bed. We plan to test this concept further in a second set of experiments (supplemental to the work currently supported in this project) using a 50m long reach in the 2.5 m wide channel at St. Anthony Falls Laboratory. The larger spatial scale and controlled changes in sediment feed will produce a nonuniform transport field that will provide a far more extensive opportunity to evaluate deposition and evacuation of sand among large roughness elements. In addition, the data set will provide an opportunity to test the sand routing (i.e. sand mass conservation) algorithm of the 1d routing model, in addition to the transport algorithm.

Table 1. Summary of run parameters and results

Ru n	Q (l/s)	Qs (g/s)	U (m/s)	Runtime (h)	Fr	R_o	Run type	Result
0	98	75	0.81	2.2	0.40	0.36	F-110	no significant bed
6a	97	200	0.80	0.8	0.40	0.37	F-110	no significant bed
3	66	75	0.56	2.0	0.28	0.52	F-110	target bed
8	60	33	0.50	2.5	0.26	0.58	F-110	target bed
12	60	75	0.50	1.3	0.25	0.58	F-110	target bed
14	66	41	0.55	2.5	0.28	0.53	F-110	target bed
6b	92	200	0.76	1.1	0.38	0.39	F-110	target bed
1	53	75	0.45	2.1	0.23	0.64	F-110	dune formed
2	71	75	0.59	2.0	0.30	0.49	F-110	dune formed
4	79	200	0.67	1.3	0.34	0.44	F-110	dune formed
5	88	200	0.73	1.0	0.36	0.40	F-110	dune formed
7	53	33	0.45	2.5	0.23	0.64	F-110	dune formed
13	71	43	0.59	2.2	0.30	0.49	Lakeland	target bed
15	66	20	0.55	2.0	0.28	0.53	Lakeland	target bed
16	79	46	0.66	3.0	0.33	0.44	Lakeland	target bed
17	93	179	0.78	1.3	0.39	0.38	Lakeland	target bed
9	63	33	0.53	1.0	0.27	0.55	Seeded bed (color)	slow deflation of bed
10	93	75	0.77	0.1	0.39	0.38	Seeded bed (color)	rapid deflation of bed
11	66	75	0.55	1.1	0.28	0.53	Seeded bed (Lakeland)	slow deflation of bed

Table 2. Summary of data collected and analyses.

Data	Analysis	Progress
ADV measurements	Characterize velocity profile, turbulence intensities, and Reynolds stresses	Preliminary analysis complete, need to redo after filtering data
Suspended sediment samples	Profiles of suspended sediment concentration	Completed
"	Suspended sediment grain size for comparison with bed samples and feed sediment size distribution	To be completed
"	Suspended sediment color to determine degree of mixing, and pattern of dune deflation for the seeded-bed runs	To be completed
Bed topography measurements	Determine average bed elevation and total bed volume	Preliminary analysis complete
Bed sediment samples	Grain size for comparison with grain size of suspended material	To be completed
Bed photographs	Use with topography measurements for more detailed measure of bed volume if needed	To be completed as needed
Video	Observations of sediment movement	To be completed as needed

References

- Andrews, E.D., Johnston, C.E., Schmidt, J.C., and Gonzales, M., 1999, Topographic evolution of sand bars, in Webb, R.H., Schmidt, J.C., Marzolf, G.R., and Valdez, R.A. (eds.), *The Controlled Flood in Grand Canyon*: Washington, D.C., American Geophysical Union, Geophysical Monograph 110, p. 117-130.
- Hazel, J.E., M. Kaplinski, R.A. Parnell, M.F. Manone, A.R. Dale, 1999, Topographic and bathymetric changes at thirty-three long-term study sites, in Webb, R.H., Schmidt, J.C., Marzolf, G.R., and Valdez, R.A. (eds.), *The Controlled Flood in Grand Canyon*, Washington, D.C., American Geophysical Union, Geophysical Monograph 110, p.161-183.
- Melis, T, Korman, J., and Walters, C.J. 2002a, Challenges in Assessing the Effects of Experimental Flow Regimes from Glen Canyon Dam on Fine Sediment Storage and Native Fish Populations in the Colorado River in Grand Canyon, Fall 2002 AGU meeting.

- Melis, T, Topping, T.J., Rubin, D.M. and Agrawal, Y. C, 2002b, Recent Innovations in Monitoring Suspended-Sediment Mass Balance of the Colorado River Ecosystem Below Glen Canyon Dam: A laser-Based Approach, . Fall 2002 AGU meeting.
- Rubin, D.M., D.J. Topping, J.C. Schmidt, J.E. Hazel, M. Kaplinski, and T.S. Melisa, 2002, Recent sediment studies refute Glen Canyon Dam hypothesis, EOS, Transactions, American Geophysical Union, v. 83, n. 25, p. 277-278.
- Topping, D.J., D.M. Rubin, L.E. Vierra Jr., 2000a, Colorado river sediment transport, 1, Natural sediment supply limitation and the influence of Glen canyon Dam, Water Resources research, v. 36, n. 2, p. 515-542.
- Topping D. J., D.M. Rubin, J.M. Nelson, P.J. Kinzel III, I.C. Corson, 2000b, Colorado river sediment transport, 2, Systematic bed-elevation and grain-size effects of sand supply limitation, Water Resources research, v. 36, n. 2, p. 543-570.
- Wiele, S.M., Graf, J.B., and Smith, J.D., 1996, Sand deposition in the Colorado River in the Grand Canyon from flooding of the Little Colorado River: Water Resources Research, v. 32, p. 3579-3596.
- Wiele, S.M., 1997, Modeling of flood-deposited sand distributions for a reach of the Colorado River below the Little Colorado River, Grand Canyon, Arizona, U.S. Geological Survey Water Resources Investigation Report.
- Wiele, S.M., Andrews, E.D., and Griffin, E.R., 1999, The effect of sand concentration on depositional rate, magnitude, and location, in Webb, R.H., Schmidt, J.C., Marzolf, G.R., and Valdez, R.A. (eds.), The Controlled Flood in Grand Canyon: Washington, D.C., American Geophysical Union, Geophysical Monograph 110, p. 131-145.
- Wiele, S.M. and Torizzo, M., Modeling of sand deposition in archeologically significant reaches of the Colorado River in Grand Canyon, USA, Bates, P., Lane, S., and Ferguson, R. (eds.) Environmental Computational Fluid Dynamics, accepted for publication and Director approved.
- Wiele, S.M. and Torizzo, M., Director approved, A stage-normalized function for the synthesis of stage-discharge relations for the Colorado River in Grand Canyon, Arizona, US Geological Survey Water Resources Report.

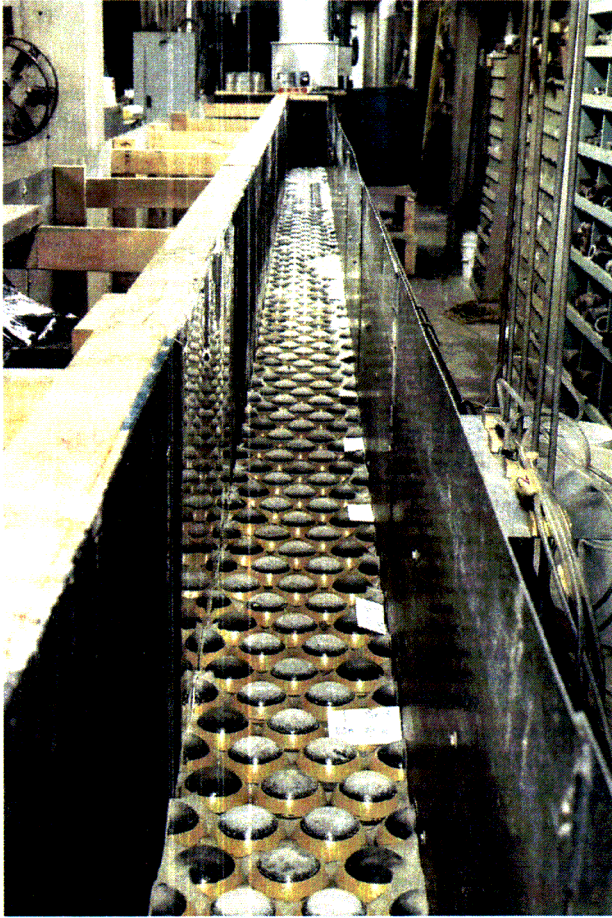


Figure 1. Photograph of flume looking upstream.

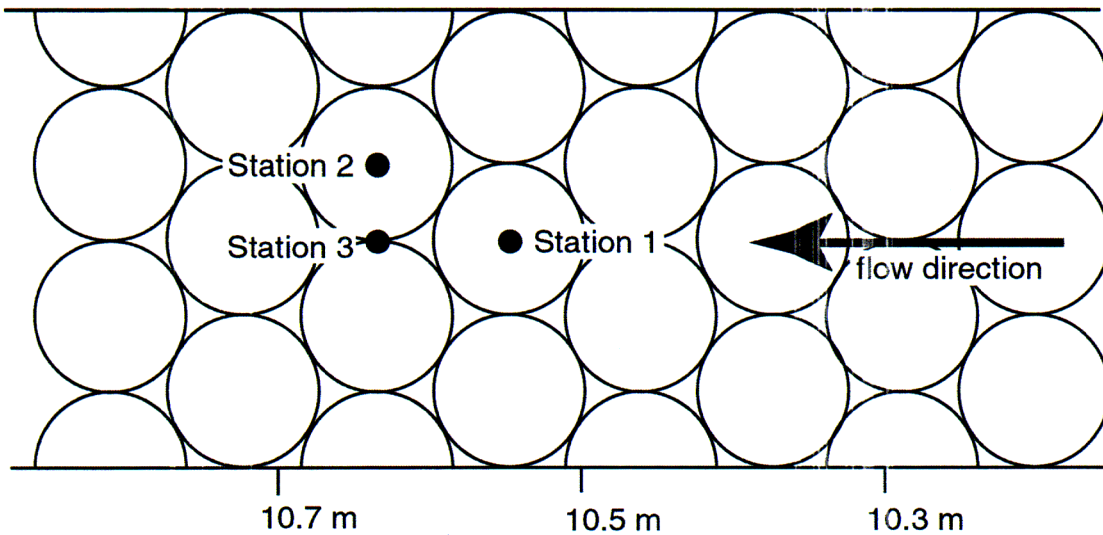


Figure 2. Sketch showing velocity and sediment sampling stations. Velocity profiles were measured at each of the stations. Suspended sediment samples were collected at Station 1.

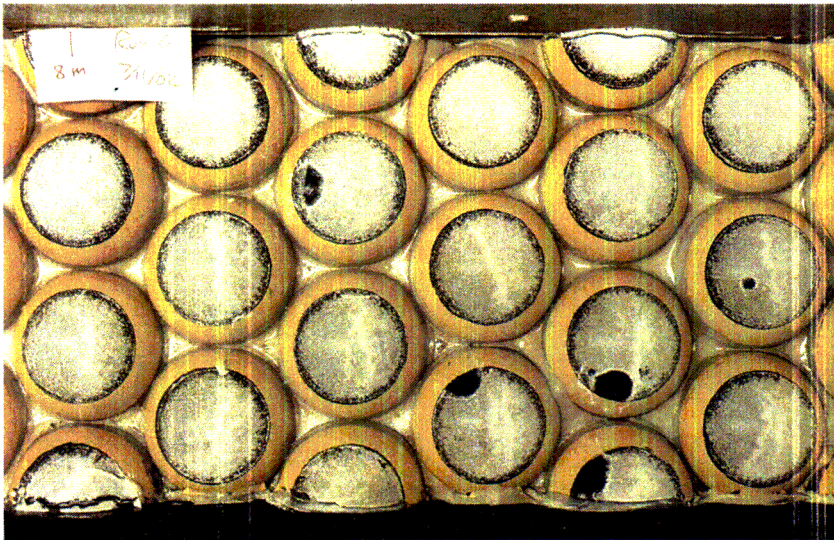


Figure 3. Photograph showing example of run with no significant sand bed (Run 0 at a distance of 8.0 m).

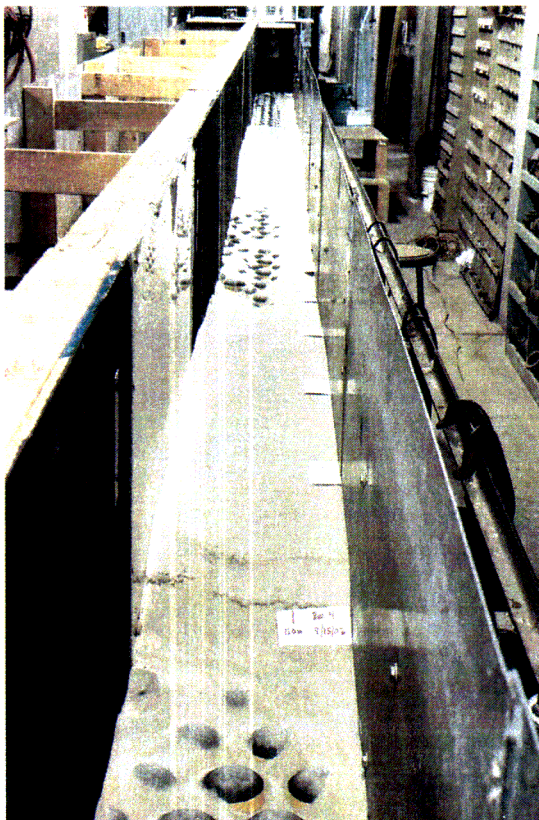


Figure 4. Photograph showing example of run with abundant sand aggradation, forming dunes (Run 4, looking up-flume).



Figure 5. Photograph of flume bed showing example of a run with sand deposition limited primarily to hemisphere interstices (Run 8, 7.5 m).

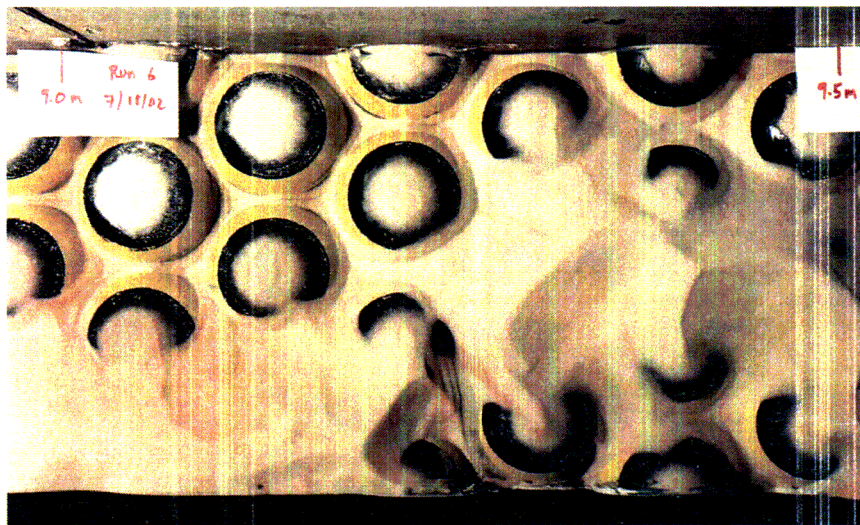


Figure 6. Photograph of flume bed showing example of a run with some sand aggradation, but with mean bed elevation below sphere tops and no dune formation.

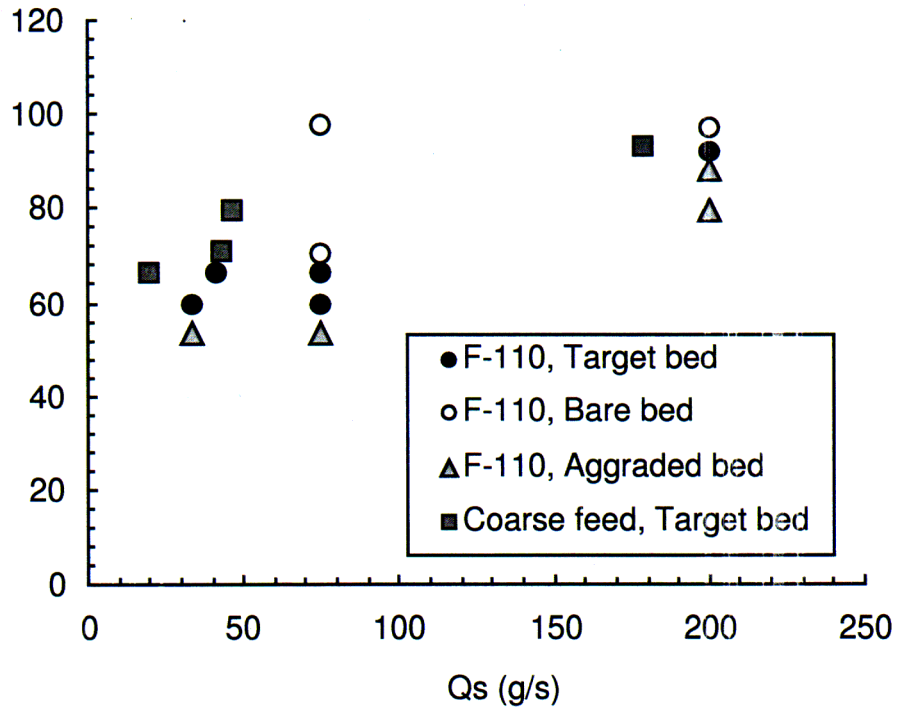


Figure 7. Plot of sediment feed rate (Q_s) and flow rate (Q) uniform transport runs. For Q_s of 75 g/s and 200 g/s, a narrow range of Q produces a “target” sediment bed with deposition of sand among the sphere interstices, but without massive aggradation and dunes. The coarse “Lakeland” sediment feed requires a larger discharge to deposit a target bed.

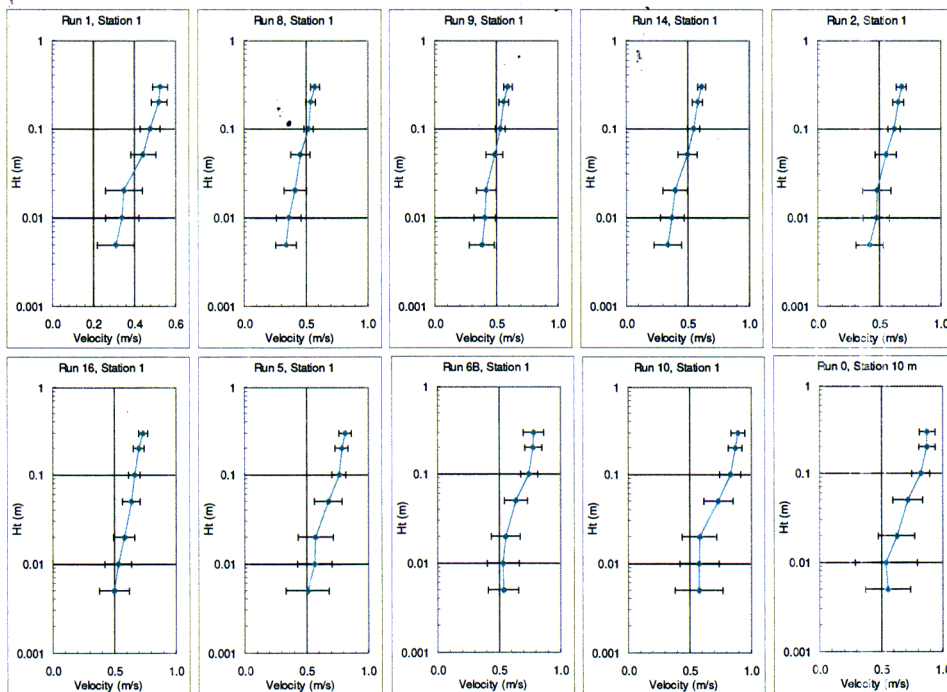


Figure 8. Profiles of mean streamwise velocity collected at sample station 1 (center of flow over hemisphere top) for each flow condition (Table 1). Plots are arranged from left to right in order of increasing flow rate.

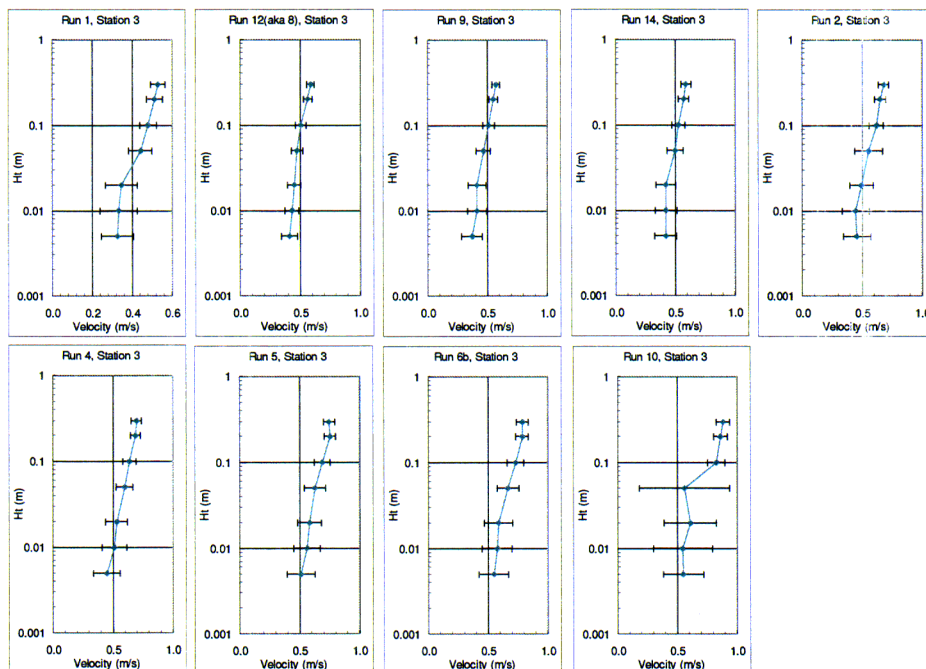


Figure 9. Profiles of mean streamwise velocity collected at sample station 3 (center of flow over interstices) for each flow condition (Table 1). Plots are arranged from left to right in order of increasing flow rate. The flow for Run 0 was not sampled at this location.

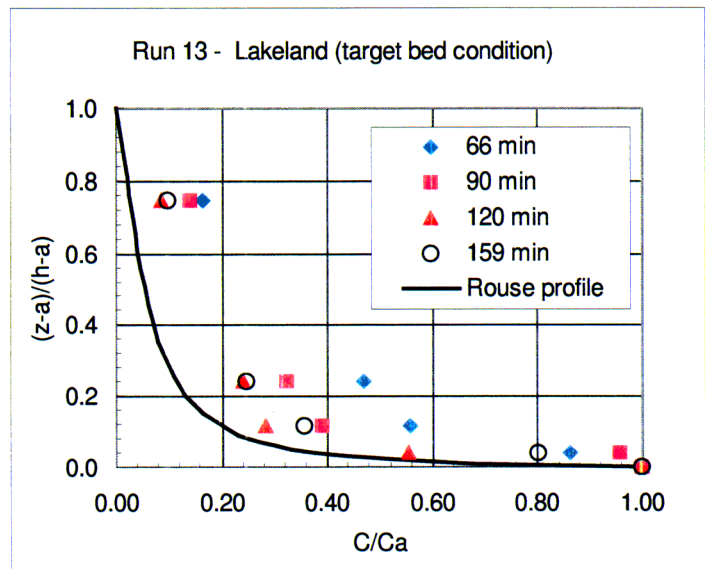
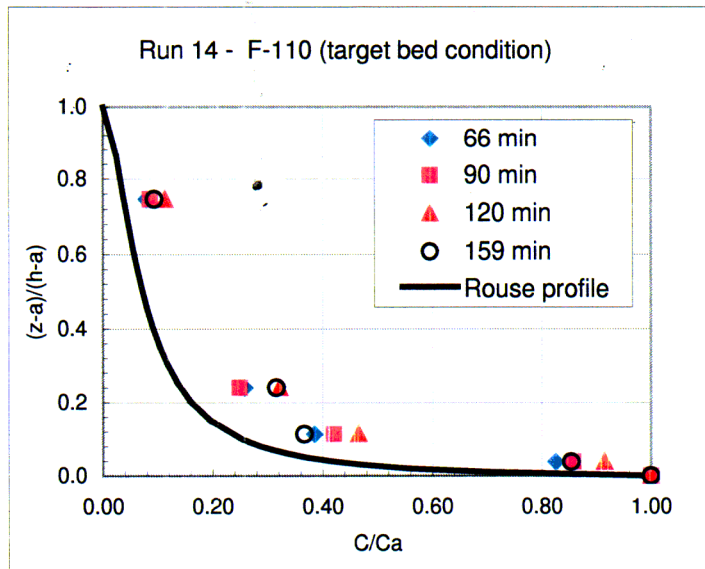


Figure 10. Examples of profiles of suspended sediment concentrations compared to predicted Rouse distribution for a reference elevation of 0.5 cm. $(Z-a)/(h-a)$ is normalized height above the bed and C/Ca is concentration normalized by the concentration at the reference elevation.

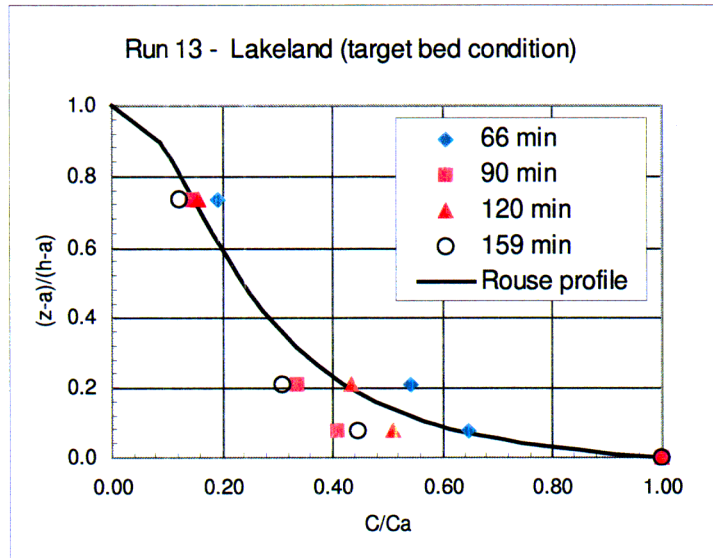
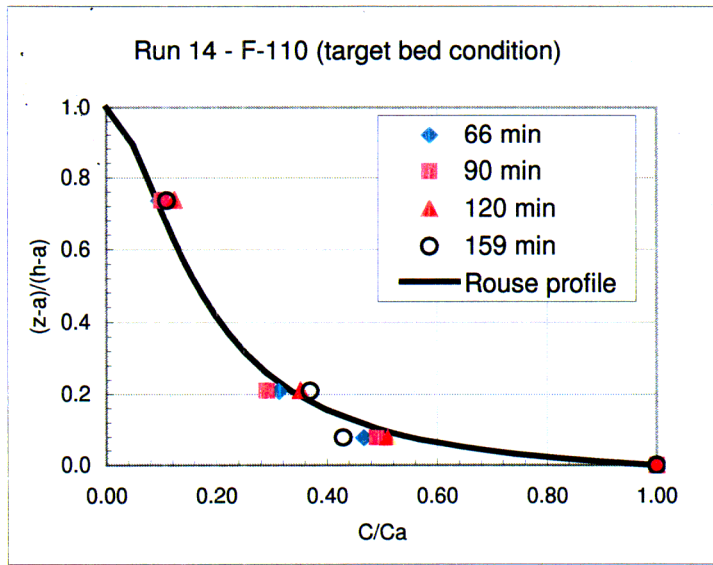


Figure 11. Examples of profiles of suspended sediment concentrations compared to predicted Rouse distribution for a reference elevation of 2.0 cm. $(Z-a)/(h-a)$ is normalized height above the bed and C/Ca is concentration normalized by the concentration at the reference elevation.

Reynolds stress and near-bed concentrations at 2 cm
above hemisphere tops

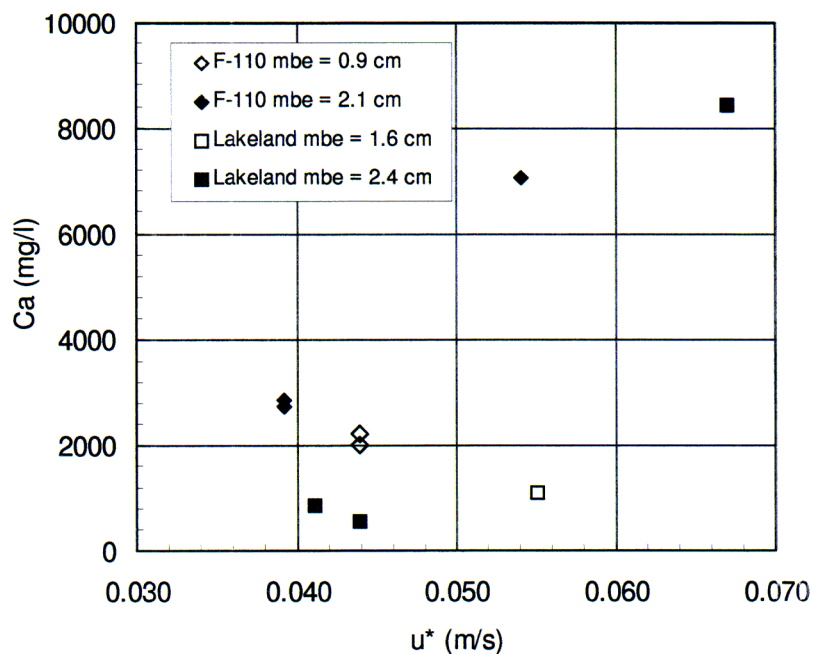


Figure 12. Plot showing the measured concentration of suspended sand collected at 2 cm over the hemisphere top as a function of the shear velocity u^* calculated from the Reynolds stress for the same position in the velocity profile. The data points are categorized by sediment feed grain size and mean sand bed elevation (mbe). The mbe is the average centerline thickness of sand in the hemisphere interstices. Only data from runs with a target mean sand bed elevation are included.